# Synchrotron infrared spectroscopy of the pressure-induced insulator-metal transitions in glassy $As_2S_3$ and $As_2Se_3$

Viktor V. Struzhkin, Alexander F. Goncharov, Razvan Caracas, Ho-kwang Mao, and Russell J. Hemley
*Geophysical Laboratory, Carnegie Institution of Washington, 5251 Broad Branch Road NW, Washington, DC 20015, USA*
(Received 22 January 2008; revised manuscript received 27 March 2008; published 29 April 2008)

Optical reflectivity and absorption measurements of glassy $As_2S_3$ and $As_2Se_3$ from 0.18 to 1.4 eV to 57 GPa reveal closure of the optical gap in both materials. The transition to the metalliclike response is continuous with pressure. The insulator-metal transition can be understood in terms of the delocalization of nonhybridized S and Se *p* states (lone pairs), as supported by the optical reflectivity data and theoretical calculations that show delocalization and evolution of three-dimensional electronic states in crystalline $As_2Se_3$.

DOI: 10.1103/PhysRevB.77.165133 PACS number(s): 78.30.Ly, 74.72.Jt, 75.30.Et, 75.50.Ee

## I. INTRODUCTION

Disordered systems based on chalcogenide glasses have attracted considerable attention due to their unusual photoelastic coupling properties[1] and athermal photomelting phenomena.[2] $As_2S_3$ and $As_2Se_3$ chalcogenide glasses are extensively studied examples of disordered systems (see e.g., Ref. 3), which preserve short-range order (SRO) and medium-range order (MRO) of their crystalline counterparts and have similar electronic structure (Fig. 1). The structure of the relevant crystalline polymorphs is shown in Fig. 2. The disordered state can be considered as retaining locally its crystalline counterpart's (Fig. 2) valence bond lengths and bond angles, which are just slightly distorted. However, it may also contain a substantial amount of broken bonds or "irregular" As-As and S-S (Se-Se) bonds, which contributes to the degree of disorder in these systems. The actual concentrations of these "defects" depend on the sample preparation techniques. The local distortions of bond lengths and angles destroy long-range order (LRO) and create a disordered state. However, the electronic structure remains quite similar in disordered glassy state and crystalline materials, as evidenced by the photoelectron spectroscopy and reflectivity studies.[4,5]

The salient feature of the electronic structure of these materials is the existence of lone-pair electron states, which do not participate in chemical bonding and are located on S (Se) atoms. The lone-pair states are quite localized in chalcogenide glasses, forming narrow bands that can be considered as "impurity" bands[4] (Fig. 1). This explains the common feature of chalcogenide glasses to have a Fermi level pinned in the middle of the gap between this filled quasi-impurity band consisting of lone-pair *p* states and antibonding (empty) *p* states, which form a conduction band.[4] The energy bands of a disordered solid would have an electronic density of states similar to the crystalline form, however, the low-density tails in the density of states and transport properties will be determined by the mobility edge[6] instead of the band edge in crystalline materials.

Previous high-pressure studies show that the energy gap closes at a rate of 0.1–0.2 eV/GPa (from absorption edge data[7–9]), and metallic conductivity is observed at 30 GPa for $As_2Se_3$.[9] However, no infrared studies have been done so far on these systems close to the metal-insulator transition. In this study, we document the pressure evolution of the band gap from absorption and reflectivity spectra in the IR spectral range through the insulator-metal transition. Our optical data indicate that the transition to metallic states in these systems is continuous at room temperature, without observable jumps in spectroscopic properties, which is in agreement with earlier resistivity data.[9] Our findings are not compatible with the behavior expected for a classical Mott-type insulator-metal transition. The optical methods used in this study allow a better understanding of the details of the insulator-metal transition, in particular, the crucial role of the delocalization of lone-pair electrons at the transition. The experimental data can be understood based on the theoretical calculations for

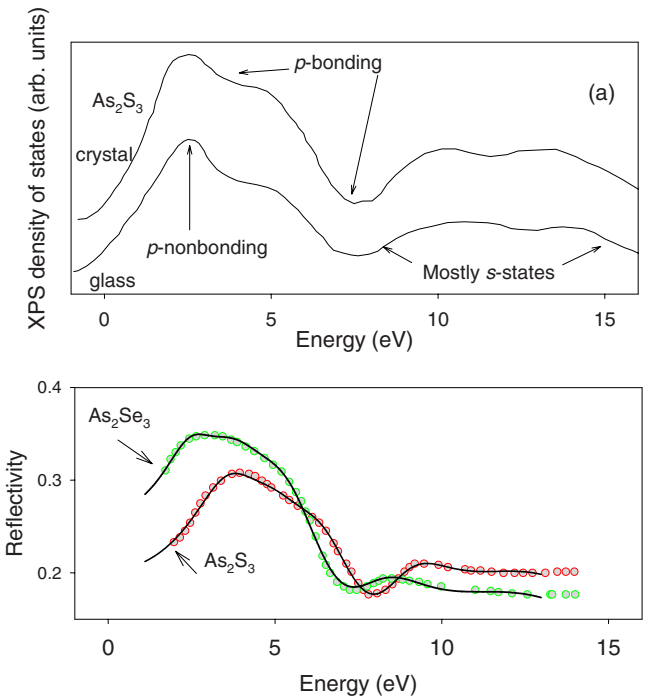


FIG. 1. (Color online) (a) Electronic spectra of crystalline and covalently bonded disordered (glassy) $As_2S_3$ according to x-ray photoemission spectroscopy measured in Ref. 4. We also indicate the distribution of the electronic states following the general considerations of Ref. 4. The reflectivity spectra from Ref. 5 (symbols) and Lorentz oscillator fits (solid lines, see text for details) are shown in the lower panel.

 

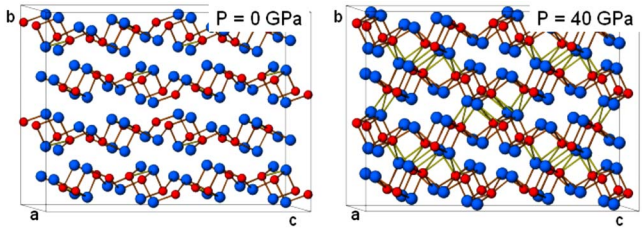


FIG. 2. (Color online) Structure of $P2_1/c$ crystalline $As_2S(Se)_3$. The disordered or glassy state can be locally considered as retaining its crystalline counterpart's SRO and partially MRO: valence bond lengths, and bond angles are just slightly distorted, and the layered structure is partially preserved (Refs. 29 and 30).

the prototype crystalline $As_2Se_3$ material, which supports the notion of similar SRO and MRO in crystalline and glassy $As_2Se_3$ and $As_2S_3$.

## II. EXPERIMENT

The samples used in the experiments were high purity glasses prepared by the methods described in Ref. 3. To prepare thin slabs, we used two quartz plates, so that samples were melted between the plates and then cooled down in air. This technique allowed us to prepare samples with thickness ranging from 2 to 10 $\mu$m, which are suitable for reflectivity/absorbance studies in diamond anvil cells. The IR absorption/reflectivity spectra were measured at room temperature at 600–12 000 $cm^{-1}$ (~0.075–1.4 eV) with a synchrotron radiation by using a Nicolet 750 Fourier transform infrared spectrometer equipped with a $CaF_2$ beam splitter and a mercury cadmium telluride detector[10] at beamline U2A at the NSLS, Brookhaven National Laboratory. The sample sizes were about 50–70 $\mu$m, we used NaCl as a pressure medium, and the high pressure chamber was about 120–150 $\mu$m in diameter. We used type Ia diamonds with 400 $\mu$m flat culets and rhenium gaskets. The use of type Ia diamonds limited our spectral range to 0.18 eV on the low-energy side. The reference transmission spectra were taken near the sample through the pressure medium, and for the reflectivity spectra, we used a reflection from the inner diamond-air interface as a reference. We measured pressure by using $R_1$ fluorescence from small ruby chips inside the sample chamber.[11]

## III. EXPERIMENTAL RESULTS

Representative reflectivity and absorption spectra of $As_2Se_3$ are shown in Fig. 3; we obtained similar data for $As_2S_3$. The reflectivity spectra do not contain any sharp features and are smooth, except for a few features at higher pressures arising from the stressed diamond anvils in the region of the multiphonon absorption in diamond. A common feature of the spectra is the monotonic increase in the reflectance with increasing pressure. We fitted the experimental spectra by using a Drude–Lorentz oscillator model, which is a standard tool in analyzing the optical response of solids[12] under pressure. Since we know the bulk features of the electronic structure and specific electronic states involved in the

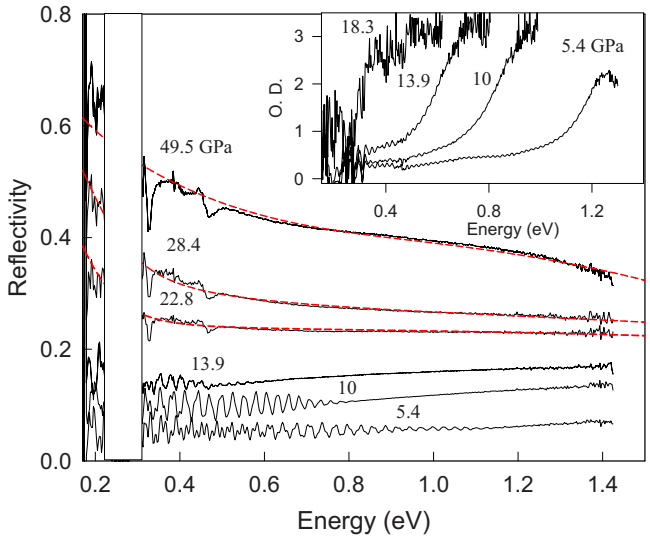


FIG. 3. (Color online) Reflectivity and absorption spectra of $As_2Se_3$. The region of second-order absorption in the diamond anvils at 0.25–03 eV is not accessible. The red dashed lines are Drude–Lorentz fits in the metallic phase.

optical transitions, we can initially estimate the number, strength, and position of the Lorentz oscillators needed to model our spectra.[12] For our materials, we need to include optical transitions to the conduction band (CB) from $s$ states (~10 eV below CB), bonding $p$ states (5–7 eV below CB), and nonbonding lone-pair $p$ states (~4 eV below CB).[4] These transitions can be modeled with several Lorentz oscillators and a Drude term to describe free charge carriers. We fitted the ambient pressure optical response from Ref. 5 by using the oscillators described above (we used a total of four oscillators to describe broad $p$ bonding and $s$ states shown in Fig. 1) and used the resulting starting parameters. We further assumed that the positions of the oscillators describing bonding $p$ states and $s$ states are pressure independent (we allowed the $p$-oscillator widths to vary), and we estimated their strength under pressure by using the density change calculated by using compressibility data from Ref. 13. The position, strength, and width of the lone-pair oscillator under pressure was adjusted to fit the reflectivity spectra. The fits described well the bulk of the reflectivity data. A few examples of these fits for $As_2Se_3$ are shown in Fig. 3. To fit the spectra at high pressures (above 20 GPa for $As_2Se_3$ and above 44 GPa for $As_2S_3$), we introduced the Drude contribution, which was enhanced by increasing pressure. The strength of the Drude contribution is shown in Fig. 4 and is estimated as $(\frac{\omega_p^D}{\omega_p^L})^2 \sim N_D/N_L$ (plasma frequency $\omega_p = \sqrt{4\pi Ne^2/m}$, $N_D$ is the Drude-type electron density, and $N_L$ is lone-pair-type electron density).

The energy gap in Fig. 4 was measured at the absorption level $\alpha = 5 \times 10^3$ $cm^{-1}$. The absorption coefficient was estimated by using the sample thickness, as measured at normal pressure (the thickness was not corrected for the compressibility of the sample; we estimate that this assumption introduced a maximum error of about 0.02 eV at the highest pressure of absorption measurements, which is comparable to the symbol size in Fig. 4). The optical gap $E_g$ measured by ab-

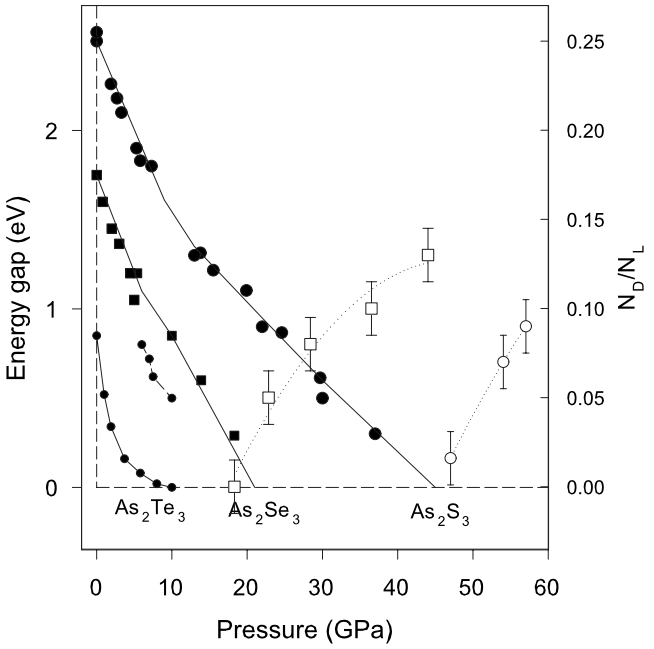


FIG. 4. Pressure dependence of the energy gap in $As_2S_3$ (large closed circles, left axis) and $As_2Se_3$ (large closed squares, left axis) from absorption measurements. Absorption data below 10 GPa for $As_2S_3$ are from Ref. 8. Absorption data below 7 GPa and energy gap from transport measurements (small circles connected with dotted line, left axis) for $As_2Se_3$ are from Ref. 9. The gap for $As_2Te_3$ from transport measurements in Ref. 31 (small circles connected by solid line, left axis) is shown for comparison. Drude contribution to reflectivity is shown for $As_2S_3$ (large open circles, right axis) and $As_2Se_3$ (large open squares, right axis).

sorption shows different slopes at low and high pressures for both $As_2Se_3$ and $As_2S_3$ (Fig. 4). A kink in $E_g(P)$ dependence is clearly visible around 5–10 GPa. We relate this kink to the changes in the glass compression, when the interlayer van der Waals forces between As-S(Se) layers become comparable to intralayer forces. This changes the compression pattern in the glass: As-S(Se) bonds undergo stronger compression because of the stiffening of softer interlayer regions under pressure above 5–10 GPa. Consequently, the splitting between the antibonding $p$ states (within the conduction bands) and the bonding $p$ states (within the valence bands) increases and, thus, slows down the closure of the optical gap $E_g$ under pressure, which agrees with our observations (Fig. 4). This behavior is consistent with the disappearance of the first sharp diffraction peak in $As_2S_3$, which is arguably related to the interlayer spacing.[14] Thus, these glasses acquire a more three-dimensional character at a sufficiently high pressure.

## IV. THEORY: BAND STRUCTURE OF COMPRESSED CRYSTALLINE $As_2Se_3$

To understand the driving forces of the insulator-metal transitions, we computed the evolution of the electronic properties of crystalline $As_2Se_3$ under pressure by using the local density approximation (LDA) of the density-functional

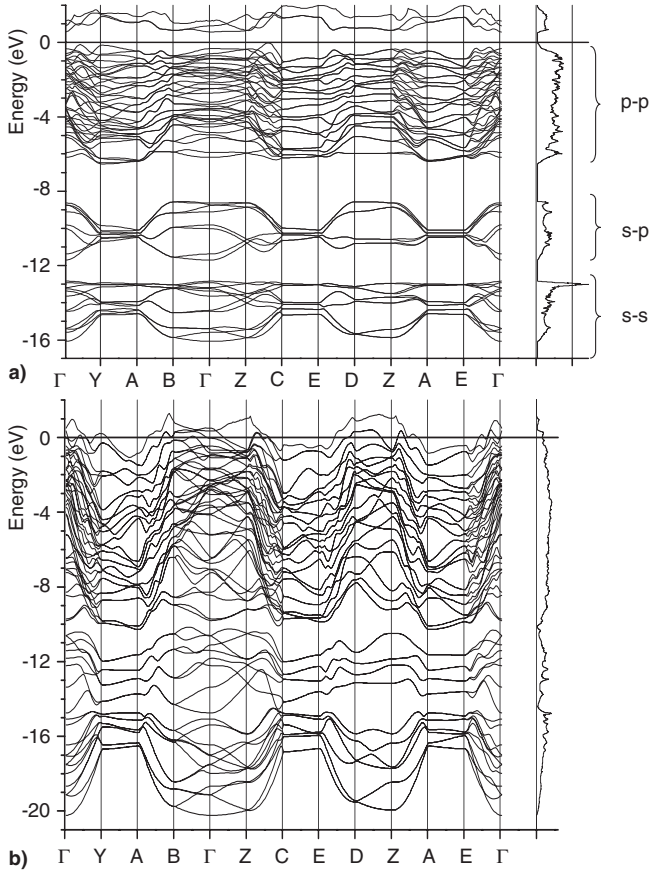


FIG. 5. Electronic band structure and density of states of the crystalline $As_2S(Se)_3$ computed at 0 and 45 GPa. $As_2Se_3$ is a low-dimensional insulator at low pressures and a three-dimensional metal at high pressures. $Y=(1/2\ 0\ 0)$, $A=(1/2\ 1/2\ 0)$, $B=(0\ 1/2\ 0)$, $Z=(0\ 0\ 1.2)$, $C=(1/2\ 0\ 1/2)$, $E=(1/2\ 1/2\ 1/2)$, and $D=(0\ 1/2\ 0)$.

theory,[15,16] as implemented in the ABINIT package.[17] $As_2Se_3$ has $P2_1/c$ symmetry and its structure is built of $[As_2Se_3]_n$ layers stacked parallel to (010) (Fig. 2). The interatomic bonds are stronger within these layers and weaker between the layers. The interlayer space hosts the lone pairs of the $p$ electrons of As and Se. We relaxed the lattice parameters and atomic degrees of freedom in the structure from zero to 45 GPa by using the Broyden–Fletcher–Goldfarb–Shanno minimization,[18] which was modified to take into account the total energy as well as gradients.[19]

At zero pressure, the crystalline $As_2Se_3$ is insulating [Fig. 5(a)]. Its electronic band structure is characterized by three groups of bands which, in increasing order of energy, correspond to $s$-$s$, $s$-$p$, and $p$-$p$ hybridizations. These groups are separated by electronic gaps. The bands are weakly dispersive perpendicular to the layering of the structure along the [010] directions, e.g., the $Y$-$A$, $C$-$E$, $A$-$E$, $B$-$\Gamma$, and $D$-$Z$ paths. The bands are more dispersive along the other directions. This is consistent with a low-dimensional (i.e., quasi-two-dimensional) solid, where the electrons are confined in the $[As_2Se_3]_n$ layers. Under pressure, the bonding between the atoms within the neighboring layers is strengthened as the distance between the (010) layers decreases; the lone pairs are delocalized and the $p$-$p$ hybridizations are en-

hanced. This increases the dimensionality of the structure, the bands become more dispersive, and the electronic gap closes due to electron delocalization [Fig. 5(b)]. The closure of the gap is continuous. For the crystalline $As_2Se_3$, we obtain an insulator-metal transition corresponding to the LDA gap closure at around 10 GPa. This theoretical insulator-metal transition pressure is underestimated when compared to the experimental data (Fig. 4) due to combined usual LDA underestimations of both band gap values and unit cell volume.

## V. DISCUSSION

Despite substantial and remarkable progress in recent decades, detailed understanding of many aspects of disordered solids still remains a challenge to both experiment and theory. The most characteristic property of these systems is the absence of translational symmetry, which makes it impossible to apply the Bloch theorem. The absence of the translational symmetry and of the long-range order in disordered solids does not mean, however, that they also lack SRO or MRO. In fact, many experimental techniques can be used to study static SRO and MRO in disordered systems.[9] One of the most studied topics in disordered materials is an insulator-metal transition, which is often referred to as a Mott–Anderson transition.[6] This transition deals with the delocalization of the electrons in a random potential and is also necessarily related to the long-range correlations in such disordered systems.[20] Another interesting property of disordered materials is superconductivity, which develops close to the metal-insulator transition[21] and may be driven by nonconventional mechanisms (negative $U$ intrinsic defects) in these systems.[22]

The nature of the insulator-metal transition in the disordered systems studied here is distinctly different from the ideal classical picture of the Mott–Anderson transition.[20] We have no data on the transport properties of $As_2S_3$ through the metal-insulator transition, but we do have data on $As_2Se_3$ to 30 GPa (Ref. 9) showing conductivity of about $\sigma(20\ \text{GPa}) \sim 100\ \Omega^{-1}\,\text{cm}^{-1}$, which is slightly lower than the minimum metallic conductivity $\sigma_{min}=\text{const}\times e^2/\hbar a \sim 250-1000\ \Omega^{-1}\,\text{cm}^{-1}$[16] (here, const=0.025–0.1, $e$ is the electron charge, and $a$ is the distance between the atoms). In contrast to that, the conductivity in $As_2Te_3$ is close to $\sigma_{min}$ at 10 GPa, where it becomes metallic according to transport measurements of activation energy.[9] We note here that in all these systems, we have the pseudogap in the density of states due to the fact that mobility edges of the valence and conduction bands do not overlap close to the metal-insulator transition while the sample is still an insulator even when the band edges are brought together by pressure effect. In general, the positions of the mobility edges depend on the width of the band tails, which we expect to increase from Te to Se and further to S because the pressure-energy scale extends in that sequence. Thus, we would expect larger pseudogap existence regions for Se than for Te and even larger pseudogap pressure regions for S. Apparently, low-temperature transport measurements are required close to the insulator-metal transition to establish the detailed behavior and to observe discontinuities (if any) in the conductivity.

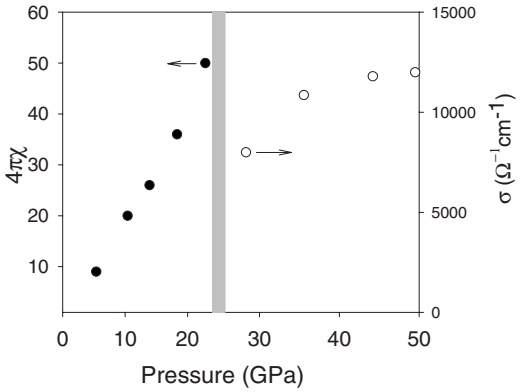


FIG. 6. Electronic susceptibility $\epsilon_1-1=4\pi\chi$ (closed symbols, left axis) in the insulating phase and conductivity (open symbols, right axis) in the metallic phase as follows from the Drude–Lorentz model fits for $As_2Se_3$.

To compare our results to well studied disordered systems, we have plotted in Fig. 6 the electronic susceptibility $\epsilon_1-1=4\pi\chi$ and conductivity, as follows from the Drude–Lorentz fits to the reflectivity data for $As_2Se_3$. The electronic susceptibility diverges when approaching the transition pressure from the insulating side, which is consistent with the extrapolation of the lone-pair oscillator frequency to zero at the transition. The details of the behavior of the conductivity could not be accurately followed near the transition, especially, the existence of the minimum metallic conductivity could not be addressed in this study, however, the general behavior is consistent with the stress-induced insulator-metal transition in phosphorus-doped silicon (as shown in Fig. 2 of Ref. 23).

## VI. CONCLUSIONS

While doping-induced insulator-metal transitions are relatively well studied and both continuous[23] and discontinuous[24] scenaria for the transition have been proposed, relatively few systems have been studied in detail under high pressures close to the insulator-metal transition regime. A continuous pressure-induced insulator-metal transition was suggested in the $FeSi_{1-x}Ge_x$ Kondo system by Mani *et al.*[25] A nonreversible pressure-induced insulator-metal transition has been observed in SiO,[26] which is possibly due to the delocalization of lone-pair electrons. Quite often, an insulator-metal transition under pressure is accompanied by a discontinuous change in the sample volume (first order phase transition),[27] which does not allow to consider pressure (volume) as a continuous parameter. It appears that the amorphous chalcogenide glasses studied here are continuously tuned by pressure and provide a perfect model system for studying the insulator-metal transition in disordered solid materials. The optical methods used in this study provide important details of the insulator-metal transition, in particular, the delocalization of lone-pair electrons at the transition. The experimental data can be understood based on the theoretical calculations for the prototype crystalline $As_2Se_3$ material, which supports the notion of similar SRO

and MRO in crystalline and glassy $As_2Se_3$ and $As_2S_3$. Further low-temperature studies are required, e.g., of transport properties in these novel pressure-induced metallic glasses to compare their behavior to existing theoretical predictions for metal-insulator transitions in disordered solids[28] and nonconventional superconductivity mechanisms.[22]

In summary, we have measured synchrotron IR reflectivity and absorption spectra of disordered chalcogenide glasses $As_2Se_3$ and $As_2S_3$ up to the metal-insulator transition. The transition pressures determined from the closure of the optical gap from the absorption measurements and from the development of the free-electron-like Drude response in reflectivity agree very well. We observe that the slope of the pressure dependence of the gap decreases in both glasses, which is consistent with the expected transition of the system to a more three-dimensional-like behavior above 5–10 GPa. The optical and resistivity[9] data are supported by first-principles calculations and indicate that the transition to metallic states in these systems is continuous and arises through lone-pair electron delocalization and *p*-band broadening, without observable jumps in spectroscopic or transport properties. Thus, the transition in these systems is unlikely a Mott-type insulator-metal transition.

## ACKNOWLEDGMENTS

This work was supported by the NSF-DMR 0508988, EAR 06-49658 (COMPRES), DOE-NNSA under Contract No. DE-FC03-03NA00144, and Department of Energy under Grant No. DE-FG02-02ER45955. The NSLS is supported by DOE-BES under Contract No. DE-AC02-98CH10886.

[1] P. Krecmer, A. M. Moulin, R. J. Stephenson, T. Rayment, M. E. Welland, and S. R. Elliott, Science **277**, 1799 (1997).
[2] H. Hisakuni and K. Tanaka, Science **270**, 974 (1995).
[3] B. T. Kolomietz, J. Phys. Colloq. **42**, No. C4, 887 (1981).
[4] S. G. Bishop and N. J. Schevchik, Phys. Rev. B **12**, 1567 (1975).
[5] R. Zallen, R. E. Drews, R. L. Emerald, and M. L. Slade, Phys. Rev. Lett. **26**, 1564 (1971).
[6] N. F. Mott, *Metal-Insulator Transitions*, 2nd ed. (Taylor & Francis, London, 1990).
[7] V. V. Struzhkin, Sov. J. Glass Phys. Chem. **15**, 658 (1989).
[8] J. M. Besson, J. Cernogora, and R. Zallen, Phys. Rev. B **22**, 3866 (1980).
[9] S. Minomura, in *Solid State Physics under Pressure*, edited by S. Minomura (Terra Scientific, Tokyo, 1985), p. 275.
[10] R. J. Hemley, A. F. Goncharov, R. Lu, V. V. Struzhkin, M. Li, and H. K. Mao, Nuovo Cimento Soc. Ital. Fis., B **20**, 539 (1998).
[11] H. K. Mao, J. Xu, and P. M. Bell, J. Geophys. Res. **91**, 4673 (1986).
[12] U. Venkateswaran, K. Syassen, H. Mattausch, and E. Schönherr, Phys. Rev. B **38**, 7105 (1988).
[13] K. Tanaka, Solid State Commun. **60**, 295 (1986).
[14] K. Tanaka, J. Non-Cryst. Solids **90**, 363 (1987).
[15] P. Hohenberg and W. Kohn, Phys. Rev. **136**, B864 (1964).
[16] W. Kohn and L. J. Sham, Phys. Rev. **140**, A1133 (1965).
[17] X. Gonze, J.-M. Beuken, R. Caracas, F. Detraux, M. Fuchs, G.-M. Rignanese, L. Sindic, M. Verstraete, G. Zerah, F. Jollet, M. Torrent, A. Roy, M. Mikami, Ph. Ghosez, J.-Y. Raty, and D. C. Allan, Comput. Mater. Sci. **25**, 478 (2002).
[18] W. H. Press, B. P. Flannery, S. A. Teukolsky, and W. T. Vetterling, *Numerical Recipes—The Art of Scientific Computing* (Cambridge University Press, Cambridge, 1989).
[19] X. Gonze, Phys. Rev. B **54**, 4383 (1996).
[20] P. W. Anderson, Phys. Rev. **109**, 1492 (1958).
[21] I. V. Berman, N. V. Brandt, I. E. Kostyleva, S. K. Pavlov, V. I. Sidorov, and S. M. Chudinov, JETP Lett. **43**, 62 (1986).
[22] P. W. Anderson, Phys. Rev. Lett. **34**, 953 (1975).
[23] T. F. Rosenbaum, R. F. Milligan, M. A. Paalanen, G. A. Thomas, R. N. Bhatt, and W. Lin, Phys. Rev. B **27**, 7509 (1983).
[24] A. Möbius, C. Frenzel, R. Thielsch, R. Rosenbaum, C. J. Adkins, M. Schreiber, H.-D. Bauer, R. Grötzschel, V. Hoffmann, T. Krieg, N. Matz, H. Vinzelberg, and M. Witcomb, Phys. Rev. B **60**, 14209 (1999).
[25] A. Mani, A. Bharathi, and Y. Hariharan, Phys. Rev. B **63**, 115103 (2001).
[26] A. Pesach, R. Shuker, and E. Sterer, Phys. Rev. B **76**, 161102(R) (2007).
[27] M. P. Pasternak, W. M. Xu, G. Kh. Rozenberg, R. D. Taylor, G. R. Hearne, and E. Sterer, Phys. Rev. B **65**, 035106 (2001).
[28] P. A. Lee and T. V. Ramakrishnan, Rev. Mod. Phys. **57**, 287 (1985); M. Imada, A. Fujimori, and Y. Tokura, *ibid.* **70**, 1039 (1998); K.-S. Kim, Phys. Rev. B **73**, 235115 (2006); P. Lombardo, R. Hayn, and G. I. Japaridze, *ibid.* **74**, 085116 (2006).
[29] E. Tarnow, A. Antonelli, and J. D. Joannopoulos, Phys. Rev. B **34**, 4059 (1986).
[30] A. A. Vaipolin, Sov. Phys. Crystallogr. **10**, 509 (1966).
[31] N. Sakai and H. Fritzsche, Phys. Rev. B **15**, 973 (1977).